Thermo-responsive release of curcumin from micelles prepared by self-assembly of amphiphilic P(NIPAAm-co-DMAAm)-b-PLLA-b-P(NIPAAm-co-DMAAm) triblock copolymers

ARTICLE *in* INTERNATIONAL JOURNAL OF PHARMACEUTICS · SEPTEMBER 2014

Impact Factor: 3.65 · DOI: 10.1016/j.ijpharm.2014.09.029 · Source: PubMed

6 AUTHORS, INCLUDING:

Yanfei Hu
Istituto Italiano di Tecnologia
12 PUBLICATIONS **148** CITATIONS
SEE PROFILE

Vincent Darcos
Université de Montpellier
40 PUBLICATIONS **633** CITATIONS
SEE PROFILE

Su-Ming Li
European Institute of Membranes
154 PUBLICATIONS **6,871** CITATIONS
SEE PROFILE

International Journal of Pharmaceutics 476 (2014) 31–40

Contents lists available at ScienceDirect

International Journal of Pharmaceutics

journal homepage: www.elsevier.com/locate/ijpharm

Thermo-responsive release of curcumin from micelles prepared by self-assembly of amphiphilic P(NIPAAm-*co*-DMAAm)-*b*-PLLA-*b*-P(NIPAAm-*co*-DMAAm) triblock copolymers

Yanfei Hu [a], Vincent Darcos [a], Sophie Monge [b], Suming Li [a,c,*], Yang Zhou [d], Feng Su [d]

[a] Institut des Biomolécules Max Mousseron, UMR CNRS 5247 – Equipe Biopolymères Artificiels, Université Montpellier I, 15 Avenue Charles Flahault, BP 14491, 34093 Montpellier Cedex 5, France
[b] Institut Charles Gerhardt, UMR 5253CNRS-UM2-ENSCM-UM1 – Equipe Ingénierie et Architectures Macromoléculaires, Université Montpellier II, cc1702, Place Eugène Bataillon, 34095 Montpellier Cedex 5, France
[c] Institut Europeen des Membranes, UMR CNRS 5635, University of Montpellier 2, 34095 Montpellier, France
[d] College of Chemical Engineering, Qingdao University of Science and Technology, 266042 Qingdao, China

ARTICLE INFO

Article history:
Received 24 July 2014
Received in revised form 19 September 2014
Accepted 22 September 2014
Available online 24 September 2014

Keywords:
Thermo-responsive
Micelle
Self-assembly
Poly(L-lactide)
Poly(*N*-isopropylacrylamide)
Curcumin

ABSTRACT

Thermo-responsive micelles are prepared by self-assembly of amphiphilic triblock copolymers composed of a poly(L-lactide) (PLLA) central block and two poly(*N*-isopropylacrylamide-*co*-*N*,*N*-dimethylacrylamide) (P(NIPAAm-*co*-DMAAm)) lateral blocks, using solvent evaporation/film hydration method. The resulting micelles exhibit very low critical micelle concentration (CMC) which slightly increases from 0.0113 to 0.0144 mg mL^{-1} while the DMAAm content increases from 31.8 to 39.4% in the hydrophilic P(NIPAAm-*co*-DMAAm) blocks. The lower critical solution temperatures (LCST) of copolymers varies from 44.7 °C to 49.4 °C in water as determined by UV spectroscopy, and decreases by *ca.* 3.5 °C in phosphate buffered saline (PBS). Curcumin was encapsulated in the core of micelles. High drug loading up to 20% is obtained with high loading efficiency (>94%). The LCST of drug loaded micelles ranges from 37.5 to 38.0 °C with drug loading increasing from 6.0 to 20%. The micelles with diameters ranging from 47.5 to 88.2 nm remain stable over one month due to the negative surface charge as determined by zeta potential (−12.4 to −18.7 mV). Drug release studies were performed under *in vitro* conditions at 37 °C and 40 °C, *i.e.* below and above the LCST, respectively. Initial burst release is observed in all cases, followed by a slower release. The release rate is higher at 40 °C than that at 37 °C due to thermo-responsive release across the LCST. On the other hand, micelles with lower drug loading exhibit higher release rate than those with higher drug loading, which is assigned to the solubility effect. Peppas' theory was applied to describe the release behaviors. Moreover, the *in vitro* cytotoxicity of copolymers was evaluated using MTT assay. The results show that the copolymers present good cytocompatibility. Therefore, the nano-scale size, low CMC, high drug loading and stability, as well as good biocompatibility indicate that these thermo-responsive triblock copolymer micelles present a good potential as carrier for targeted delivery of anticancer drugs.

1. Introduction

Self-assembled micelles from amphiphilic block copolymers have been widely investigated as nanocarrier for controlled release of drugs (Watanabe et al., 2006; Yang et al., 2010a; Yang et al., 2010b; Zhao and Yung, 2008). Nano-size polymeric micelles exhibit outstanding properties such as reduced side effects, improved therapeutic efficacy, selective targeting, stable storage, and prolonged blood circulation. Furthermore, polymeric micelles can achieve higher accumulation at the target site through the enhanced permeation retention (EPR) effect (Gaucher et al., 2005; Kataoka et al., 2001; Torchilin, 2001).

Curcumin, a natural polyphenol derived from curcuma longa, exhibits a wide spectrum of pharmacological activities including anti-oxidant, anti-inflammatory, anti-microbial, anti-amyloid and anti-tumor properties due to its diverse range of molecular targets (Maheshwari et al., 2006). In the past decades, it was regarded as a prominent drug for treating inflammation, cystic fibrosis,

* Corresponding author. Current address: Institut Europeen des Membranes, UMR CNRS 5635, University of Montpellier 2, 34095 Montpellier, France. Tel.: +33 467 149 121.
E-mail address: lisuming@univ-montp1.fr (S. Li).

http://dx.doi.org/10.1016/j.ijpharm.2014.09.029
0378-5173/

Alzheimer's and malarial diseases and cancer (Aggarwal et al., 2003; Agrawal and Mishra, 2009; Anand et al., 2008; Kunnumakkara et al., 2008). The therapeutic efficacy of curcumin is limited by its extremely low solubility (11 ng mL^{-1}) in water (Tonnesen, 2002). Moreover, rapid metabolism and elimination lead to poor bioactivity of curcumin (Anand et al., 2007).

Recently, polymer micelles have been used to encapsulate curcumin so as to enhance the solubility, cellular uptake and anti-tumor bioactivity (Gong et al., 2013; Gou et al., 2011; Liu et al., 2013; Song et al., 2011a; Song et al., 2011b). Micelles prepared from poly(ethylene glycol)-*b*-poly(ε-caprolactone) (mPEG-*b*-PCL) diblock copolymers have been largely studied for controlled delivery of curcumin. However, mPEG-*b*-PCL micelles with drug loading of 9.9% were unstable as aggregates were observed in 72 h (Gong et al., 2013). Song et al. reported the preparation, pharmaco-kinetics and distribution of curcumin loaded micelles using poly(D,L-lactide-*co*-glycolide)-*b*-poly(ethylene glycol)-*b*-poly (D,L-lactide-*co*-glycolide) (PLGA-*b*-PEG-*b*-PLGA) triblock copolymers (Song et al., 2011b). The prolongation of half-life, enhanced residence time and decreased total clearance indicate that the micelles could prolong the acting time of curcumin *in vivo*. Nevertheless, both the drug loading (6.4%) and encapsulation efficiency (70%) need to be improved. Polymer-conjugate micelles were prepared to enhance the curcumin loading, but only 7.5% cumulative drug release was obtained after 60 h as drug release is controlled by degradation of micelles (Yang et al., 2012).

Among the polymeric micelles described in literature, none is sensitive to environmental changes. It is well known that different from normal tissues, tumor has a particularly high temperature (~40 °C) (Chilkoti et al., 2002). Therefore, thermo-sensitive polymeric micelles based on poly(*N*-isopropylacrylamide) (PNIPAAm) with a lower critical solution temperature (LCST) at 32 °C attracted much attention for targeted stimuli-responsive drug release (Chang et al., 2011; Kim et al., 2000; Rezaei et al., 2014; Wei et al., 2009; Xu et al., 2013). The hydrophilic PNIPAAm outer shell becomes hydrophobic by increasing the temperature above the LCST. The selective accumulation of micelles at a specific site could be enhanced as a result of enhanced micelle adsorption to cells by hydrophobic interactions between the polymeric micelles. Therefore, thermo-responsive micelles could deliver the drugs *via* a stimuli-responsive targeting process at tumor sites. In addition, nano-scaled thermo-responsive polymeric micelles could combine the passive targeting by EPR effect and active targeting by stimuli response, thus leading to accelerated release of the encapsulated drug at desired sites.

To the best of our knowledge, no thermo-responsive curcumin encapsulated polymeric micelles have been reported, so far. In this work, thermo-responsive micelles were prepared from copolymers composed of a poly(L-lactide) (PLLA) central block and two poly(*N*-isopropylacrylamide-*co*-*N*,*N*-dimethylacrylamide) (P(NIPAAm-*co*-DMAAm)) lateral blocks, using solvent evaporation/film hydration method. Curcumin was loaded in the core of micelles during the fabrication procedure. Drug release studies were realized under *in vitro* conditions in a pH 7.4 phosphate buffer at 37 and 40 °C. The cytotoxicity of micelles was evaluated using MTT assay. The results are reported herein in comparison with literature data.

2. Materials and methods

2.1. Materials

α,ω-Bromopropionyl PLLA (Br-PLLA-Br) with degree of polymerization (DP) of 40 was prepared as previously reported (Hu et al., 2013). Tris(2-dimethyl aminoethyl) amine (Me_6TREN), copper (I) chloride (CuCl), *N*-isopropylacrylamide (NIPAAm), *N*,*N*-dimethyl formamide (DMF), chloroform, dicholoromethane, diethyl ether, basic aluminum oxide, Tween 80, ethylenediaminetetraacetic acid tetrasodiumsalt hydrate (EDTA-Na_4·H_2O) and curcumin were obtained from Sigma–Aldrich, and used without further purification. DMAAm was obtained from Sigma–Aldrich and purified through a basic aluminum oxide column. Ultrapure water with a conductivity of 18 MΩ was produced using a Millipore
Milli-Q water system.

2.2. Synthesis of triblock copolymer

P(NIPAAm-*co*-DMAAm)-*b*-PLA-*b*-P(NIPAAm-*co*-DMAAm) triblock copolymers were prepared by atom transfer radical polymerization (ATRP) at 25 °C using a DMF/water mixture solvent as reported previously (Hu et al., 2014).

2.3. Preparation of curcumin-loaded polymer micelles

Typically, 2.51 mg curcumin and 17.53 mg copolymer T2 (Sample 2, Table 3) were dissolved in 20 mL acetone. The solvent was evaporated in rotary evaporator at room temperature to yield a membrane on the wall of the flask. After vacuum drying for 24 h, 20 mL Milli-Q water was added to the flask. Drug loaded micelles were obtained under stirring at room temperature. The micelle solution was then centrifuged at 5000 rpm for 10 min to remove unload curcumin, and the supernatant was lyophilized and stored at 4 °C before use.

2.4. In vitro *drug release*

The drug loading (DL) and encapsulation efficiency (EE) were determined as follows. 5 mg lyophilized micelles were dissolved in 5 mL acetonitrile/ammonium acetate (10 mM) mixture solution (pH 4.0). Then the solution was diluted 100 times. The concentration of curcumin was determined by UV–vis spectroscopy at 424 nm, using a previously established standard calibration curve. The DL and EE were calculated according to the following equations:

$$\mathrm{DL} = \frac{\text{weight of loaded drug}}{\text{weight of polymeric micelles}} \times 100\% \quad (1)$$

$$\mathrm{EE} = \frac{\text{weight of drug in micelles}}{\text{theoretical drug loading}} \times 100\% \quad (2)$$

Drug loaded micelles (2 mg) were dispersed in 2 mL PBS solution (pH 7.4), and then introduced into a dialysis bag (MW cut-off 3500 Daltons). The bag was placed in 10 mL PBS containing 0.5 wt% Tween80 in an incubator (Heidolph 1000) with gentle shaking (150 rpm) at 37 or 40 °C. At specific time intervals, the release medium was removed and replaced by pre-warmed (37 °C or 40 °C) fresh medium. The withdrawn solution was then diluted 10 times with pH 4.0 acetonitrile/ammonium acetate (10 mM) mixture solution for UV measurement.

2.5. In vitro *cytotoxicity assay Test*

The cytotoxicity of copolymers was evaluated by MTT assay. After UV sterilization for 5 h, the copolymer T2 was dissolved in Dulbecco's Modified Eagle's Meduim (DMEM, Hyclone products) at

Table 1
Relationship between the RGR value and cytotoxicity level.

Level	0	1	2	3	4	5
RGR (%)	≥100	75–99	50–74	25–49	1–24	0

Table 2
Properites of the P(NIPAAm-co-DMAAm)-*b*-PLA-*b*-P(NIPAAm-co-DMAAm) triblock copolymers.

Run	[PLA]/[NIPAAm]/[DMAAm]$_0$	[LA]/[NIPAAm]/[DMAAm][a]	[NIPAAm]/DMAAm[a]	$M_{n,NMR}$[a]	$M_{n,SEC}$[b]	PDI[b]
Cop T1	1/148.8/51.2	40/74/34	68.5/31.8	18300	26000	1.1
Cop T2	1/147.5/52.5	40/65/32	67.0/34.2	19700	25000	1.1
Cop T3	1/142.6/57.4	40/66/36	64.7/35.2	14300	18000	1.1
Cop T4	1/136.2/63.8	40/63/41	61.6/39.4	14500	19000	1.1

[a] Calculated by NMR.
[b] Determined by SEC.

a concentration of 6 mg mL^{-1}. Then the solution was transferred to 96-well plates (Corning costar, USA), 100 μL per well.The wells were placed in an incubator (NU-4850, NuAire, USA) at 37 °C under humidified atmosphere containing 5% CO_2 for 24 h. After incubation, the copolymer in the form of a hydrogel was used as cell culture substrate.

Murine fibrosarcoma (L929) and human lung carcinoma cell (A549) in logarithmic growth phase were harvested and diluted with DMEM medium (10% calf serum, 100 μg mL^{-1} penicillin, 100 μg mL^{-1} streptomycin) to a concentration of 1×10^5 cells mL^{-1}. 100 μLcellular solution was added in each hydrogel containing well which was then placed in the same incubator under humidified atmosphere containing 5% CO_2 at 37 °C. 100 μL fresh medium was used as the negative control, and 100 μL of 5% phenol solution as the positive control. After 2, 3 and 4 days, 20 μL 3-(4, 5-dimethylthiazol-2-yl)-2,5-diphenyltetrazolium bromide (MTT) at 5 mg mL^{-1} were added. The medium was removed after 6 h incubation, and 150 μL dimethylsulfoxide (DMSO) was added. After 15 min shaking, the optical density (OD) was measured by using a microplate reader (Elx800, BioTek USA) at 490 nm.

The relative growth ratio (RGR) was calculated by using the following equation:

$$\mathrm{RGR}(\%) = \left(\frac{\mathrm{OD}_{\text{test sample}}}{\mathrm{OD}_{\text{negative control}}}\right) \times 100 \quad (3)$$

The cytotoxicity is generally noted in 0–5 levels according to the RGR value as shown in Table 1.

The cellular morphology was observed using an Olympus CKX41 inverted microscope. After 3 days seeding, the test medium was replaced with 150 μL neutral red staining solution (NR) for 10 min at room temperature. The plates were rinsed 3 times with warm phosphate-buffered saline (PBS), and the morphology of cells adhered to the hydrogel surface was immediately observed under microscope.

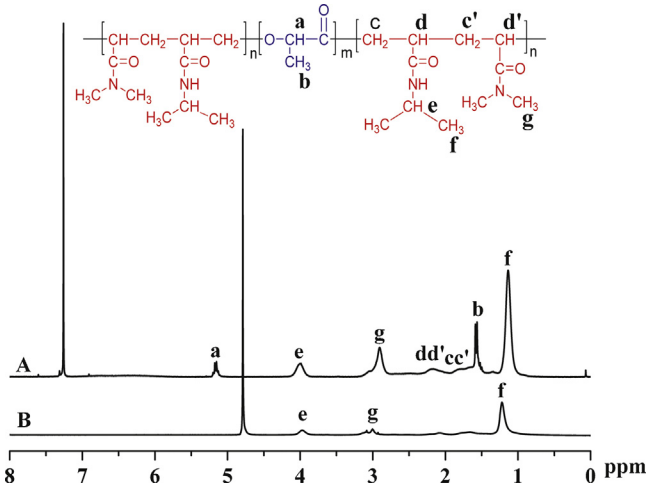

Fig. 1. ^{1}H NMR spectra of P(NIPAAm-co-DMAAm)-*b*-PLA-*b*-P(NIPAAm-co-DMAAm) triblock copolymer in (A) $CDCl_3$ and (B) D_2O at room temperature.

2.6. Characterization

2.6.1. Nuclear magnetic resonance (^{1}H NMR)

^{1}H NMR spectra were recorded on a Bruker spectrometer (AMX300) operating at 300 MHz. Chemical shift was referenced to the peak of residual non-deuterated solvents.

2.6.2. Size exclusion chromatography (SEC)

SEC measurements were performed on a Varian 390-LC equipped with a refractive index detector and two ResiPore columns (300 × 7.5 mm) at 60 °C at a flow rate of 1 mL min^{-1}. The eluent was DMF containing 0.1 wt% LiBr. Calibration was established with poly(methyl methacrylate) (PMMA) standards.

2.6.3. Fluorescence spectroscopy

The critical micellar concentration (CMC) of copolymers was determined by fluorescence spectroscopy using pyrene as a hydrophobic fluorescent probe. Measurements were carried outon an RF 5302 Shimadzu spectrofluorometer (Japan) equipped with Xenon light source (UXL-150S, Ushio, Japan). The fluorescence excitation spectra of copolymer solutions containing 6×10^{-7} M pyrene were recorded from 300 to 360 nm at an emission wavelength of 394 nm. The emission and excitation slit widths were 3 and 5 nm, respectively. The excitation fluorescence values I_{337} and I_{333}, respectively at 337 and 333 nm, were used for subsequent calculations.

2.6.4. Cloud point

The LCST was estimated from the changes in the transmittance through copolymer solutions at 1.0 mg mL^{-1} as a function of temperature. The measurements were carried out at a wavelength of 500 nm with a PerkinElmer Lambda 35 UV–vis spectrometer

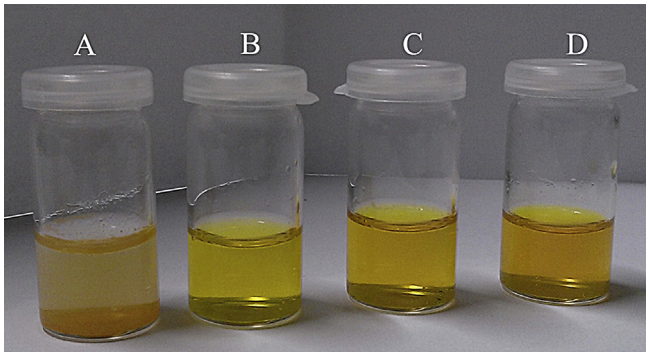

Fig. 2. Optical photographs of curcumin in different media. (A) 6.0% curcumin in H_2O; (B) 6.0% Cur–polymer micelles in PBS at 1 mg mL^{-1}; (C) 12.1% Cur–polymer micelles in PBS at 1 mg mL^{-1}; (D) 20.4% Cur–polymer micelles in PBS at 1 mg mL^{-1}.

Table 3
Characterization of triblock copolymer micelles.

Micelles	[LA]/[NIPAAm]/[DMAAm][a]	[NIPAAm]/DMAAm[a]	CMC[b] g mL^{-1}	D[c] (nm)	PDI[c]	LCST[d] (°C)	LCST[e] (°C)	ZP[f] (mv)
Cop T1	40/74/34	68.2/31.8	11.3	36.7	0.11	44.7	41.4	−18.7
Cop T2	40/65/32	65.8/34.2	13.1	38.6	0.11	45.6	42.1	−12.4
Cop T3	40/66/36	64.7/35.2	13.7	41.2	0.14	45.9	42.5	−15.3
Cop T4	40/63/41	61.6/39.4	14.4	44.1	0.17	49.4	46.2	−16.4

[a] By ^{1}H NMR.
[b] By fluorescence spectroscopy.
[c] By DLS.
[d] By UV spectroscopy in deionzed water.
[e] By UV spectroscopy in PBS.
[f] By Zetasizer Nano-ZS.

equipped with a Peltier temperature programmer PTP-1 + 1. The temperature ramp was 0.1 °C min^{-1}.

2.6.5. Dynamic light scattering (DLS) and zeta-potential (ZP)

The size and zeta-potential of micelles were determined by using Zetasizer Nano-ZS (Malvern Instrument Ltd., UK) equipped with a He–Ne laser (λ = 632.8 nm). Polymer solutions at 1.0 mg mL^{-1}were filtered through a 0.45 μm PTFE microfilter before measurements.

2.6.6. Transmission electron microscopy (TEM)

TEM experiments were carried out on a JEOL 1200 EXII instrument operating at an acceleration voltage of 120 kV. The samples were prepared by dropping a polymer solution at 1.0 mg mL^{-1}onto a carbon coated copper grid, followed by air drying.

2.6.7. Inductively coupled plasma-mass spectrometey (ICP-MS)

The residual copper content in the copolymers was quantified using a ThemoFinnigan Element XR sector field ICP-MS previously calibrated using copper solutions in water. Typically, ICP-MS samples were prepared by dissolution of the copolymers in nitric acid. The solution was then heated to fully decompose the polymer. Afterwards, the samples were dissolved in 10 mL deionized water before analysis to determine the copper concentration. Each sample was analyzed four times.

3. Results and discussion

3.1. Synthesis of triblockcopolymers

A series of P(NIPAAm-*co*-DMAAm)-*b*-PLA-*b*-P(NIPAAm-*co*-DMAAm) triblock copolymers were successfully synthesized by ATRP as described in a previous work (Hu et al., 2014). The DP of PLLA macroinitiator is 40, while that of NIPAAm and DMAAm ranges from 63 to 74, and from 32 to 41, respectively (Table 2). Various NIPAAm/DMAAm ratios were used to tailor the properties of the resulting copolymers. The molecular weights determined by SEC ($M_{n,SEC}$) range from 18,000 to 26,000 g mol^{-1}with narrow dispersity ($Đ$ = 1.1), whereas the molecular weights determined by ^{1}HNMR ($M_{n,NMR}$) are lower. $M_{n,SEC}$ values are obtained with respect to PMMA standards, and are generally higher than absolute molecular weights.

The chemical structure of triblock copolymers was characterized by ^{1}H NMR spectroscopy. As shown in Fig. 1A, the peaks at 1.1 and 4.0 ppm were attributed respectively to the methyl (H_f, CH_3) and the methine protons (H_e, CH) adjacent to the amine moiety of NIPAAm units. The signal at 2.9 ppm is assigned to the methyl proton (H_g, CH_3) of the DMAAm units. The signals at 1.6 and 5.2 ppm are characteristic of the methyl (H_b) and methine protons (H_a, CH) of PLLA. The composition of copolymers, the DP of NIPAAm and DMAAm in the hydrophilic block, and the molecular weight (M_n) of copolymers were calculated from the integrations of the methine protons of lactyl units at 5.1 ppm, the methine protons of NIPAAm units at 4.0 ppm, and the methyl protons of DMAAm at 2.9 ppm.

After polymerization, the catalyst was removed by filtration through a basic alumina column. The copolymers recovered by precipitation in diethyl ether appeared almost colorless. ICP-MS measurements showed that the copper content in the copolymers was between 1 and 3 ppm.

3.2. Characterization of polymer micelles

It is well-known that amphiphilic copolymers can form polymeric micelles by self-assembly in aqueous medium. Fig. 1B shows the ^{1}H NMR spectrum of copolymer T2 obtained in D_2O. Compared with the ^{1}H NMR spectrum in $CDCl_3$ (Fig. 2A), the peaks belonging to PLLA moieties at 5.2 and 1.6 ppm totally disappear in D_2O. This finding evidences the aggregation of copolymers into micelles with the PLLA block in the core and P(NIPAAm-*co*-DMAAm) blocks at the corona.

Table 4
Properties of curcumin-loaded polymer (T2) micelles.

Sample	Cur/polymer$_0$ (mg/mg)	DL[a] (%)	EE[a] (%)	LCST[b] (°C)	D[c](nm)	PDI[c]	Zeta-potential (mv)[d]	
							In water	In PBS
1	1.24/18.86	6.0	97.2	38.0	47.5	0.19	-13.9	−7.51
2	2.51/17.53	12.1	96.6	37.8	53.7	0.21	-15.5	−7.68
3	4.50/16.27	20.4	94.1	37.5	88.2	0.25	-18.1	−2.39

[a] By UV.
[b] By UV in PBS.
[c] By DLS in water.
[d] By Zeta Nano-Sizer.

The CMC is an important parameter which reflects the stability of micelles upon dilution. The lower the CMC, the higher the stability of micelles. In this work, the CMC was determined by fluorescence spectroscopy using pyrene as the probe. As shown in Table 3, the CMC of copolymers slightly increases from 0.0113 to 0.0144 mg mL^{-1} while the content of DMAAm increases from 31.8% for T1 to 39.4% for T4 in the hydrophilic part. In fact, the CMC is dependent on different factors such as the composition, the hydrophilic to hydrophobic ratio, the molecular weight, etc. The DMAAm units are more hydrophilic than NIPAAm ones. Thus, higher DMAAm contents lead to higher CMC. The very low CMC values indicate the strong tendency of copolymers toward formation of micelles, which is of major importance for the stability of micelles in the bloodstream after injection induced dilution (Yokoyama et al., 1991).

The LCST of copolymers was determined by light transmission measurements using UV spectroscopy. As shown in Table 3, the LCST value in distilled water increases from 44.7 to 49.4 °C with

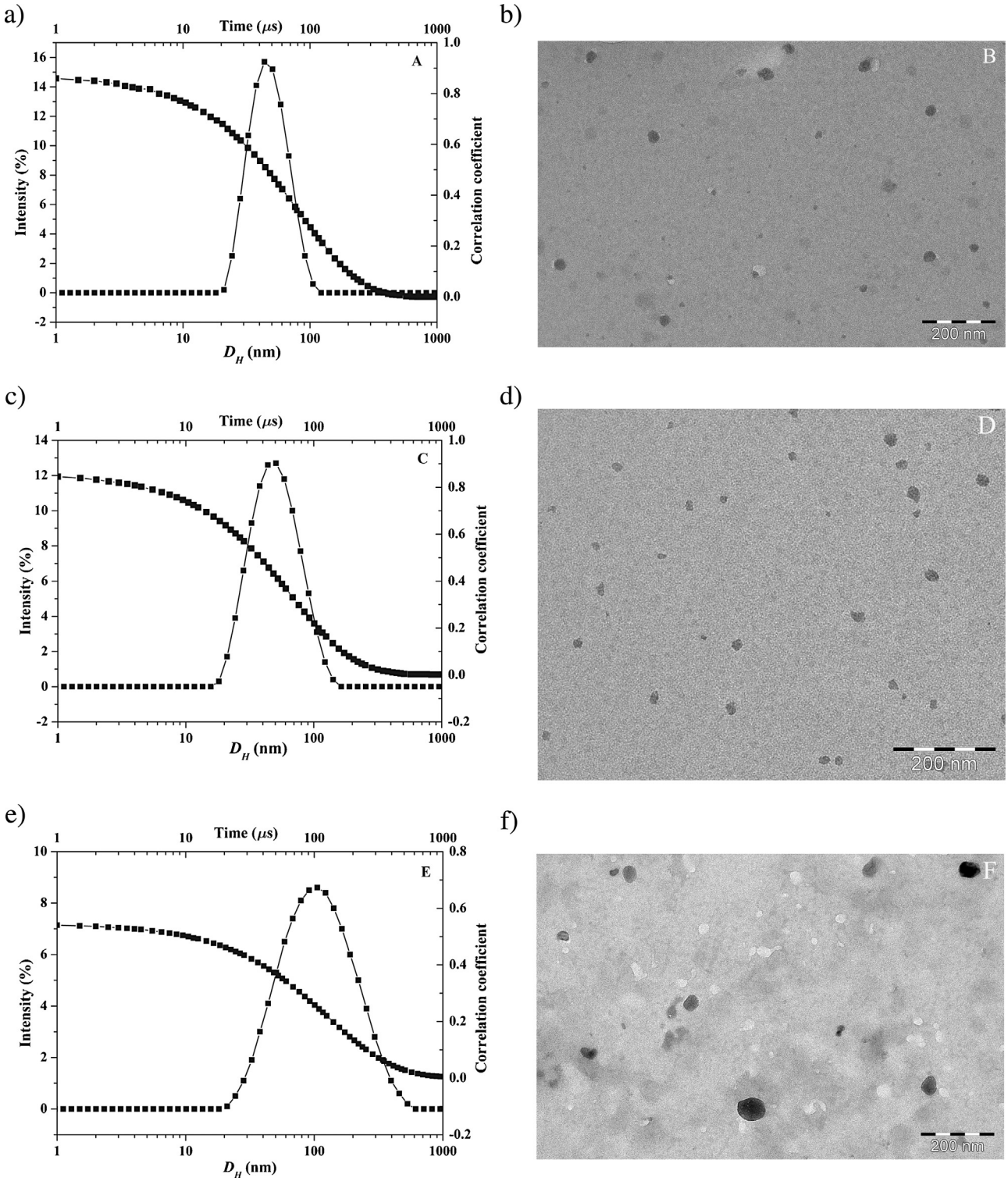

Fig. 3. DLS spectra and TEM micrographs of Cur–polymer micelles. (A) and (B): Sample 1 (DL = 6.0%); (C) and (D): Sample 2 (DL = 12.1%); (E) and (F): Sample 3 (DL = 20.4%).

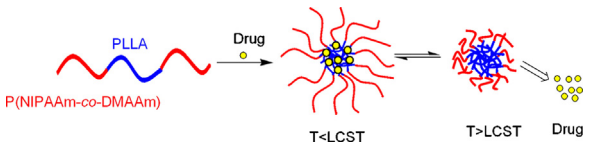

Fig. 4. Illustration of drug release from polymeric micelles controlled by LCST.

increasing DMAAm content in the hydrophilic blocks. LCST measurements were also performed in a pH 7.4 phosphate buffered saline (PBS) to mimic the *in vivo* conditions. A decrease of *ca*. 3.5 degrees in LCST values is observed in PBS as compared to those in distilled water.

The size and size distribution of copolymer micelles was determined by dynamic light scattering (DLS). The average diameter varies from 36.7 to 44.1 nm, and the polydispersity (PDI) from 0.11 to 0.17 with increasing DMAAm content in the hydrophilic blocks. The zeta-potential (ZP) of copolymer micelles varies in the −12.4 to −18.7 mV range. The zeta potential increases with
the increase of hydrophilic content. This finding well agrees with the structure of micelles having PLLA block in the core and P(NIPAAm-*co*-DMAAm) blocks at the corona.

3.2.1. Preparation and characterization of drug loaded micelles

Curcumin is a natural anticancer drug, but its application is limited due to poor solubility. Different ratios of curcumin and copolymer T2 were used to prepare drug loaded micelles by solvent evaporation/membrane hydration method (Table 4). After lyophilization, the micelles were dispersed in PBS solution for drug release studies.

The drug loading (DL) and loading efficiency (LE) of micelles were obtained by light transmission measurements using UV spectroscopy. When the initial drug amount increases from 1.24 to 4.50 mg with approximately the same amount of polymer, drug loading increases from 6.0 to 20.4%. The loading efficiency is above 94% in all cases (Table 4).

The curcumin-loaded micelle samples in PBS at 1.0 mg mL^{-1} are shown in Fig. 2, in comparison with a 6.0% curcumin solution in water. Curcumin remains as a sediment in water due to the poor solubility (Fig. 2A). On the contrary, a homogenous and transparent yellow solution is obtained in the case of curcumin-loaded micelles (Fig. 2B, C and D), showing that hydrophobiccurcumin was successfully loaded inside the polymeric micelles.

The effect of drug load on the micelle properties was investigated in detail (Table 4). Fig. 3 shows the DLS and TEM results of Samples 1, 2 and 3. With increase of drug load from 6.0 to 20.4%, the average size of micelles increases from 47.5 to 88.2 nm with corresponding PDI increasing from 0.19 to 0.25. This finding well agrees with literature data. In fact, Gong et al. reported an increase of size (from 21.7 to 36.2 nm) and PDI (from 0.098 to 0.259) of curcumin loaded mPEG-*b*-PCL micelles (Gong et al., 2013). The size of our micelles is larger than that of mPEG-*b*-PCL (21.7 to 36.2 nm) or PLGA-PEG-PLGA micelles (29.3 nm), probably due to higher hydrophobic to hydrophilic ratios (Gong et al., 2013; Song et al., 2011b).

TEM experiments were performed to examine the morphology of the self-assembled aggregates. As shown in Fig. 3, the curcumin-loaded micelles with DL = 6.0%, 12.1% and 20.4% are spherical in shape with an average diameter of 33, 42 and 75 nm, respectively.The size obtained from DLS is larger than that from TEM due to different experimental conditions. In fact, DLS allows determining the hydrodynamic diameter of micelles in aqueous solution, whereas TEM shows the dehydrated solid state of micelles.

The zeta potential (ZP) of curcumin-loaded micelles in water ranges from −13.9 for Sample 1 to −18.1 mV for Sample 3, indicating good micellar stability. Compared to blank polymer micelles, curcumin-loaded micelles present higher charge due to the presence of curcumin. The ZP of Samples 1, 2 and 3 decreases to −7.51, −7.68 and −2.39 mV in PBS, respectively. This significant decrease can be attributed to the ionic screening effect and clustered aggregate (Xu et al., 2013). All the samples remained homogeneously transparent over 1 month. It is known that more pronounced zeta potential values tend to stabilize particles in suspension. The electrostatic repulsion between micelles with the same electrical charge prevents aggregation of micelles (Ding et al., 2006; Feng and Huang, 2001). Thus, the negatively charged surface of micelles could help to stabilize the micelles via both the steric and electrostatic mechanisms. It is of interest to note that mPEG-PCL micelles with 9% curcumin loading remained stable for 72 h (Gong et al., 2013). On the other hand, Liu et al. reported stablem PEG-PCL micelles with small size (28.2 nm) with low zeta potential (0.41 mv) (Liu et al., 2013). The stability was attributed to

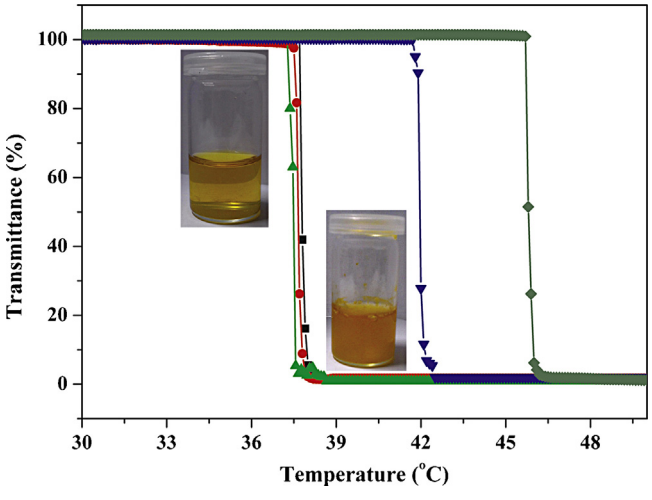

Fig. 5. Phase transitions (LCST) of cur–polymer micelles at 1 mg mL^{-1} determined by UV–vis spectroscopy. ◆DL = 0 in water; ▼DL = 0 in PBS (pH 7.4); ■ DL = 6.0% in PBS (pH 7.4) ● DL = 12.1% in PBS (pH 7.4) ▲DL = 20.4% in PBS (pH 7.4).

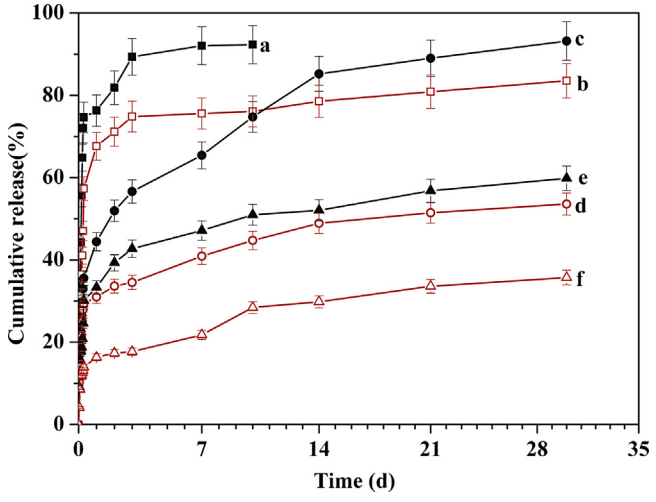

Fig. 6. Drug release profiles of cur-polymer micelles at 37 °C (red) and 40 °C (black). a and b: Sample 1 (DL = 6.0%); c and d Sample 2 (DL = 12.1%). e and f Sample 3 (DL = 20.4%). (For interpretation of the references to colour in this figure legend, the reader is referred to the web version of this article.)

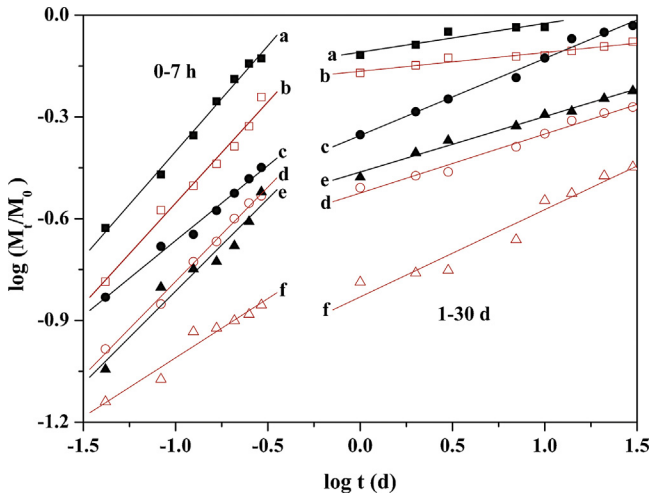

Fig. 7. Plots of theoretical fitting for curcumin release from cur-polymer micelles at 37 (red) and 40 °C (black): a and b, DL = 6%; c and d, DL = 12.1%; e and f, DL = 20.1%. (For interpretation of the references to colour in this figure legend, the reader is referred to the web version of this article.)

the stereospecific blockade of micelles although the authors did not mention the duration of micelle stability.

Both the size and zeta potential are important physicochemical properties of micelles because they determine the physical stability as well as the biopharmaceutical properties. The nano-size
(47.5–88.2 nm) of curcumin-loaded micelles allows them to escape from the reticuloendothelial system and preferentially accumulate in tumor tissues through the EPR effect (Bertrand et al., 2014; Maeda et al., 2000; Oerlemans et al., 2010; Yan et al., 2012). The charge of nanomaterials is also an important factor to affect the biocompatibility (Bertrand et al., 2014). Generally, positive charges are considered as harmful to the plasma exposure of nanomaterials since they could induce the formation of primary platelet clots (Campbell et al., 2002; He et al., 2010; Yamamoto et al., 2001). On the contrary, negative charges of micelles are beneficial to negatively charged human blood as they could enhance the binding of micelles to proteins, reduce undesirable clearance by the reticuloendothelial system such as liver, improve the blood compatibility, and thus deliver the anti-cancer drugs more efficiently to the tumor sites (He et al., 2010; Xiao et al., 2011).

3.2.2. Phase transition of curcumin loaded polymer micelles

It is well known that the drug release of thermo-responsive polymeric micelles is controlled by the phase transition (Fig. 4). The solution of triblock copolymers is transparent below the LCST. When the temperature increases above the LCST, dehydration of P(NIPAAm-*co*-DMAAm) occurs due to coil-to-globule transition, leading to precipitation of polymers and the release of drug from the matrix.

Fig. 5 shows the phase transition of various curcumin-loaded micelles in water or in PBS. The initially transparent solution of curcumin-loaded micelles becomes turbid when the temperature increases above the LCST. In the meantime, the transmittance of the solution rapidly decreases from 100% to 0.

The presence of salt greatly affects the behavior of thermo-responsive polymers. As shown in Fig. 5, the LCST of blank micelles decreases from 45.6 °C in water to 42.1 °C in PBS due to the high ionic strength in PBS and screening effect from counter-ions. The presence of phosphate leads to partial dehydration of the macromolecules and consequently to a decrease of the LCST.

The influence of drug load on the LCST was also considered in PBS. The LCST of curcumin-loaded micelles with 6.0% drug load is 38.0 °C in PBS, which is lower by 4.1 °C than that of drug free micelles (Fig. 5, Table 3). This finding is assigned to the enhanced core hydrophobicity due to encapsulated drug. Higher drug load leads to lower LCST, but the decrease is very limited. In fact, the LCST only slightly decreases from 38.0 to 37.5 °C when the drug load increases from 6.0% to 20.4%.

In addition, the phase transition intervals are very sharp (<0.5 °C) in all cases, as reported in our previous work (Hu et al., 2014). The fast phase transition favors rapid response of drug release when the micelles were delivered to the tumor site.

3.3. In vitro *drug release*

Drug release was performed under physiological conditions (PBS, pH 7.4) at 37 °C (below the LCST) and 40 °C (above the LCST), respectively. The amount of curcumin was determined from the UV–vis absorbance at 424 nm. A linear calibration curve was previously established between the UV absorbance and curcumin concentration with a correlation coefficient of 0.999 (see Fig. 1S, Supporting information).

The *in vitro* release profiles are shown in Fig. 6. The release rate of curcumin from micelles is strongly influenced by the phase transition at the LCST. The cumulative drug release at 40 °C (above LSCT) is much higher than that at 37 °C (below LCST). In all cases, burst-like release is observed. The cumulative release for Samples 1, 2 and 3 after 1 h at 40 °C is 23.6%, 14.7% and 9.0%, respectively, while it is 16.3%, 10.4% and 4.1% at 37 °C. The burst-like release at 37 °C can be attributed to the release of drug located at the interface between the core and corona of micelles. The larger burst-like release at 40 °C is attributed not only to the fast release because of phase transition above the LCST, but also to the release of drug located at the interface.

Sample 1 with 6.0% drug loading shows the fastest drug release. After the first 3 days, 74.9% and 89.3% of the loaded curcumin are released at 37 °C and 40 °C, respectively. Beyond, the release rate slows down. The cumulative release of curcumin reaches 84.0% at 37 °C after 30 days and 92.3% at 40 °C after 10 days. The release rate is slower for Sample 2 with initial drug loading of 12.1%. The cumulative release is 85.2% and 48.9% after 14 days, and 91.1% and 53.6% after 30 days at 40 °C and 37 °C, respectively. Sample 3 with initial drug loading of 20.4% shows the slowest drug release. After

Table 5
Release exponent (n), rate constant (k) and correlation coefficient (R^2) for drug release from cur–polymer micelles.

Sample	Time interval	40 °C			37 °C		
		n	k	R^2	n	k	R^2
Sample 1	0–7h	0.6238	1.6667	0.997	0.5969	1.1033	0.992
	1–30d	0.0843	0.7780	0.943	0.0552	0.6834	0.974
Sample 2	0–7h	0.4430	0.6002	0.995	0.5563	0.5904	0.997
	1–30d	0.22693	0.4421	0.994	0.17396	0.2990	0.991
Sample 3	0–7h	0.5444	0.5376	0.975	0.3490	0.2187	0.974
	1–30d	0.1638	0.3448	0.994	0.2576	0.1477	0.972

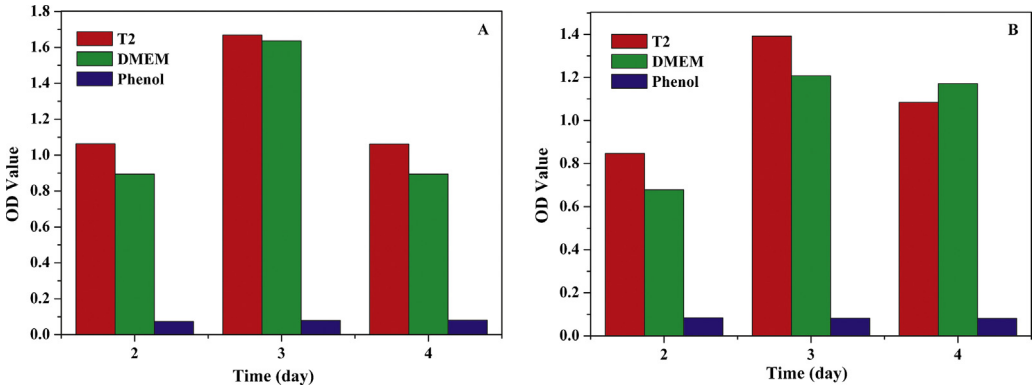

Fig. 8. Optical density values of L929 (A) and A549 (B) solutions after 2, 3 and 4 days culture in DMEM with copolymer substrate (T2), and controls (DMEM and 5% phenol).

Table 6
RGR values of copolymers T4 with A549 and L929 cells during 4 day incubation.

Cell	RGR (%)		
	2 days	3 days	4 days
L929	118.9	102.0	118.8
A549	124.9	115.2	92.6

30 days, curcumin release reaches 59.8% and 35.7% at 40 °C and 37 °C, respectively. It is noteworthy that Liu et al. reported 57% curcumin release from mPEG-PCL copolymer micelles (DL = 14.8%) after 7 days at 37 °C (Liu et al., 2013), i.e. slightly higher than the 40.9% release from Sample 2 (DL = 12.1%).

Therefore, drug release is not only dependent on the phase transition across the LCST, but also on the drug loading. In fact, the solubility of curcumin in the release medium is a limiting factor. Samples with higher drug loading exhibits lower release rate because of the solubility effect. It should also be noted that the LCST of curcumin-loaded micelles is dynamically changing with the release of curcumin. Theoretically, the LCST will increase up to 42.1 °C when the drug release reaches 100% for all the samples as shown in Fig. 5.

Peppas et al. proposed the following semi-empirical equation to describe the drug release mechanism from a polymeric matrix (Ritger and Peppas, 1987a,b; Siepmann and Peppas, 2012):

$$\frac{M_t}{M_0} = kt^n \tag{4}$$

$$\log\left(\frac{M_t}{M_0}\right) = n\log t + \log k \tag{5}$$

where M_t and M_0 are the cumulative amount of released drug at time t and the drug loading, respectively, k is a constant incorporating structural and geometric characteristic of the device, and n is the release exponent indicating the drug release mechanism. For spherical particles, the value of n is equal to

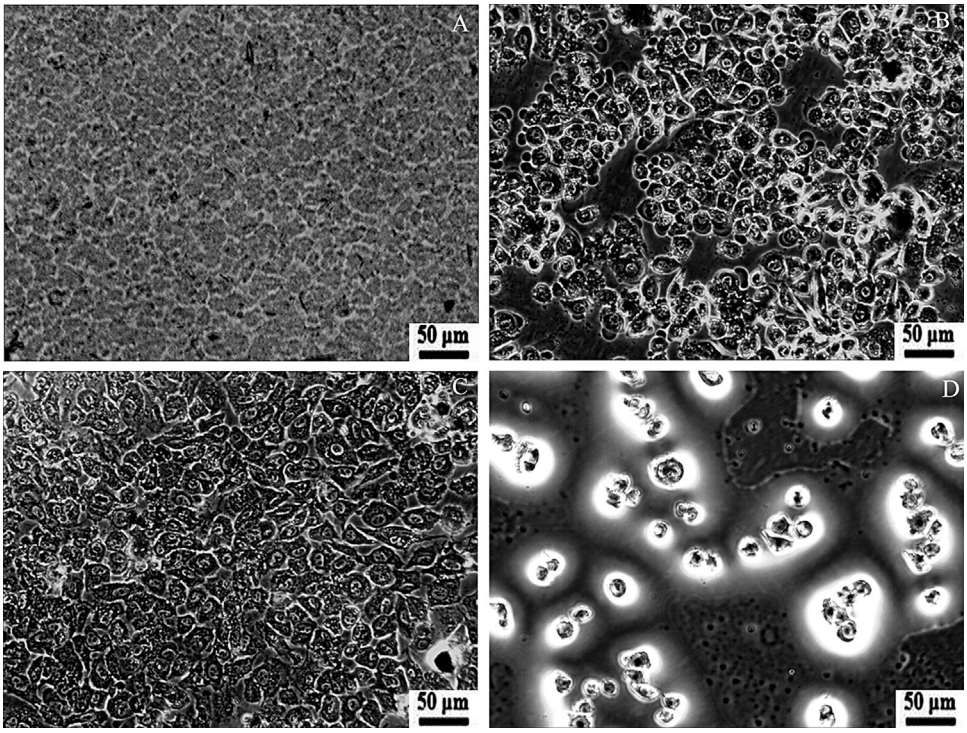

Fig. 9. Microscopic images of cells stained by NR after 3 days culture in different media: (A) copolymer T2 substrate without cell; (B) L929 cells on polymer substrate in DMEM; (C) A549 cells on polymer substrate in DMEM; (D) A549 cells in 5% phenol medium.

0.43 for Fickian diffusion, and equal to 0.85 for swelling-controlled mechanism. In contrast, $n < 0.43$ means combination of diffusion and degradation controlled release, and $0.43 < n < 0.85$ is assigned to anomalous transport mechanism.

Fig. 7 presents the theoretical fitting plots. The various release curves are divided in two stages: from 0 to 7 h and from 1 to 30 days. The fitting parameters n, k and the correlation coefficient R^2 are summarized in Table 5. For the first stage, the n values at 40 °C are in the range of 0.43 to 0.85, suggesting that the release of curcumin involves anomalous transport probably due to phase transition across the LCST. The n values of Samples 1 and 2 at 37 °C are also in the range of 0.43 to 0.85, which could be assigned to the initial burst release. The n value of Sample 3 at 37 °C is 0.349, indicating diffusion and degradation controlled release according to Peppas' theory. It might also be attributed to the highest drug loading and compact micelle structure. For the second stage, the n values in all cases are well below 0.43, suggesting a combination of diffusion and degradation controlled release. For both stages, the $k$values at 40 °C are higher than those at 37 °C, which confirms a faster drug release above the LCST due to collapse of micelles.

Therefore, the release of curcumin from thermo-responsive curcumin-loaded micelles is strongly affected by the phase transition across the LCST. Such release would favor drug accumulation at a specific tumor site where the temperature is above the LCST. Thus the micelles could combine the passive targeting by EPR effect due to the small size ranging from 47.5 to 88.2 nm, and the active targeting by thermo-responsive phase transition.

3.4. In vitro *cytocompatibility*

Curcumin is a natural polyphenolic compound with low intrinsic toxicity. The *in vitro* cytotoxicity of copolymers is evaluated by MTT assay, a widely used method for the screening of biomaterials. MTT assay is based on the reaction between MTT and mitochondrial succinate dehydrogenases in living cells to form a purple formazan which is soluble in DMSO but insoluble in water. The OD value of formazan-DMSO solution is considered to be proportional to the number of living cells.

The effects of copolymer T2 on the proliferation of L929 and A549 cells are shown in Fig. 8. In comparison with controls (DMEM medium and 5% phenol), the OD values on polymer substrate are close to those in the culture medium, and much higher than those in phenol. The RGR values (Table 6) of copolymer T2 are well above 92.6% during 4 days incubation with L929 and A549 cells, corresponding to a cytotoxicity level of 0 and 1 as defined in Table 1, thus indicating that the copolymers present no cytotoxicity.

Fig. 9 shows the morphology of cells after 3 days culture. Large number of cells died in the toxic phenol medium (Fig. 9D). On the contrary, cell adhesion and proliferation are observed on the copolymer substrate (Fig. 9B and C). Cells exhibit spindle, polygon or oval shapes, and the pseudopodium of cells stretches out. Therefore, MTT assay and cell morphology results indicate that P(NIPAAm-*co*-DMAAm)-*b*-PLLA-*b*-P(NIPAAm-*co*-DMAAm) copolymers present outstanding cytocompatibility and could be used for biomedical applications.

4. Conclusions

In this work, thermo-responsive micelles are prepared by self-assembly of P(NIPAAm-*co*-DMAAm)-*b*-PLLA-*b*-P(NIPAAm-*co*-DMAAm) triblock copolymers as drug carrier. Curcumin was used as a model drug. Compared to mPEG-*b*-PCL or PLGA-*b*-PEG-*b*-PLGA micelles, the thermo-responsive micelles described in this work present several advantages. First, lower CMC values ranging from 0.0113 to 0.0144 mg $mL^{-1}$are obtained, which should enhance the stability of micelles during long circulation in the bloodstream after injection induced dilution. Second, high curcumin loading up to 20.4% was achieved. Meanwhile, the micelles remain stable over 1 month due to the negative surface charge as shown by zeta potential measurements. Last, the micelles with sizes ranging from 47.5 to 88.2 nm could combine the passive targeting by EPR effect and thermo-responsive targeted release. Such responsive behavior will favor the release at specific tumor sites (~40 °C). Therefore, all these properties show that P(NIPAAm-*co*-DMAAm)-*b*-PLLA-*b*-P(NIPAAm-*co*-DMAAm) thermo-responsive micelles are promising as a functional drug carrier.

Acknowledgment

The authors are grateful to the China Scholarship Council for the Ph.D. fellowship of Yanfei Hu.

Reference

Aggarwal, B.B., Kumar, A., Bharti, A.C., 2003. Anticancer potential of curcumin: preclinical and clinical studies. Anticancer Res. 23, 363–398.
Agrawal, D.K., Mishra, P.K., 2009. Curcumin and its analogues: potential anticancer agents. Med. Res. Rev. 30, 818–860.
Anand, P., Kunnumakkara, A.B., Newman, R.A., Aggarwal, B.B., 2007. Bioavailability of curcumin: problems and promises. Mol. Pharm. 4, 807–818.
Anand, P., Sundaram, C., Jhurani, S., Kunnumakkara, A.B., Aggarwal, B.B., 2008. Curcumin and cancer: an old-age disease with an age-old solution. Cancer Lett. 267, 133–164.
Bertrand, N., Wu, J., Xu, X.Y., Kamaly, N., Farokhzad, O.C., 2014. Cancer nanotechnology: the impact of passive and active targeting in the era of modern cancer biology. Adv. Drug Delivery Rev. 66, 2–25.
Campbell, R.B., Fukumura, D., Brown, E.B., Mazzola, L.M., Izumi, Y., Jain, R.K., Torchilin, V.P., Munn, L.L., 2002. Cationic charge determines the distribution of liposomes between the vascular and extravascular compartments of tumors. Cancer Res. 62, 6831–6836.
Chang, C., Wei, H., Wu, D.Q., Yang, B., Chen, N., Cheng, S.X., Zhang, X.Z., Zhuo, R.X., 2011. Thermo-responsive shell cross-linked PMMA-*b*-*P*(NIPAAm-co-NAS) micelles for drug delivery. Int. J. Pharm. 420, 333–340.
Chilkoti, A., Dreher, M.R., Meyer, D.E., Raucher, D., 2002. Targeted drug delivery by thermally responsive polymers. Adv. Drug Delivery Rev. 54, 613–630.
Ding, H., Wu, F., Huang, Y., Zhang, Z.R., Nie, Y., 2006. Synthesis and characterization of temperature-responsive copolymer of PELGA modified poly(*N*-isopropylacrylamide). Polymer 47, 1575–1583.
Feng, S.S., Huang, G.F., 2001. Effects of emulsifiers on the controlled release of paclitaxel (Taxol (R)) from nanospheres of biodegradable polymers. J. Controlled Release 71, 53–69.
Gaucher, G., Dufresne, M.H., Sant, V.P., Kang, N., Maysinger, D., Leroux, J.C., 2005. Block copolymer micelles: preparation, characterization and application in drug delivery. J. Controlled Release 109, 169–188.
Gong, C.Y., Deng, S.Y., Wu, Q.J., Xiang, M.L., Wei, X.W., Li, L., Gao, X., Wang, B.L., Sun, L., Chen, Y.S., Li, Y.C., Liu, L., Qian, Z.Y., Wei, Y.Q., 2013. Improving antiangiogenesis and anti-tumor activity of curcumin by biodegradable polymeric micelles. Biomaterials 34, 1413–1432.
Gou, M.L., Men, K., Shi, H.S., Xiang, M.L., Zhang, J.A., Song, J., Long, J.L., Wan, Y., Luo, F., Zhao, X., Qian, Z.Y., 2011. Curcumin-loaded biodegradable polymeric micelles for colon cancer therapy in vitro and in vivo. Nanoscale 3, 1558–1567.
He, C.B., Hu, Y.P., Yin, L.C., Tang, C., Yin, C.H., 2010. Effects of particle size and surface charge on cellular uptake and biodistribution of polymeric nanoparticles. Biomaterials 31, 3657–3666.
Hu, Y., Darcos, V., Monge, S., Li, S., 2013. Synthesis and self-assembling of poly(*N*-isopropylacrylamide-block-poly(ι-lactide)-block-poly(*N*-isopropylacrylamide) triblock copolymers prepared by combination of ring-opening polymerization and atom transfer radical polymerization. J. Polym. Sci. Part A: Poly. Chem. 51, 3274–3283.
Hu, Y., Darcos, V., Monge, S., Li, S., Zhou, Y., Su, F., 2014. Tunable thermo-responsive P(NIPAAm-co-DMAAm)-*b*-PLLA-*b*-*P*(NIPAAm-co-DMAAm) triblock copolymer micelles as drug carriers. J. Mater. Chem. B 2, 2738–2748.
Kataoka, K., Harada, A., Nagasaki, Y., 2001. Block copolymer micelles for drug delivery: design, characterization and biological significance. Adv. Drug Delivery Rev. 47, 113–131.
Kim, I.S., Jeong, Y.I., Cho, C.S., Kim, S.H., 2000. Thermo-responsive self-assembled polymeric micelles for drug delivery in vitro. Int. J. Pharm. 205, 165–172.
Kunnumakkara, A.B., Anand, P., Aggarwal, B.B., 2008. Curcumin inhibits proliferation, invasion, angiogenesis and metastasis of different cancers through interaction with multiple cell signaling proteins. Cancer Lett. 269, 199–225.
Liu, L., Sun, L., Wu, Q., Guo, W., Li, L., Chen, Y., Li, Y., Gong, C., Qian, Z., Wei, Y., 2013. Curcumin loaded polymeric micelles inhibit breast tumor growth and spontaneous pulmonary metastasis. Int. J. Pharm. 443, 175–182.

Maeda, H., Wu, J., Sawa, T., Matsumura, Y., Hori, K., 2000. Tumor vascular permeability and the EPR effect in macromolecular therapeutics: a review. J. Controlled Release 65, 271–284.
Maheshwari, R.K., Singh, A.K., Gaddipati, J., Srimal, R.C., 2006. Multiple biological activities of curcumin: a short review. Life Sci. 78, 2081–2087.
Oerlemans, C., Bult, W., Bos, M., Storm, G., Nijsen, J.F., Hennink, W., 2010. Polymeric micelles in anticancer therapy targeting imaging and triggered release. Pharm. Res. 27, 2569–2589.
Rezaei, S.J.T., Nabid, M.R., Niknejad, H., Entezami, A.A., 2014. Folate-decorated thermoresponsive micelles based on star-shaped amphiphilic block copolymers for efficient intracellular release of anticancer drugs. Int. J. Pharm. 437, 70–79.
Ritger, P.L., Peppas, N.A., 1987a. A simple equation for description of solute releasel. Fickian and non-fickian release from non-swellable devices in the form of slabs spheres cylinders or discs. J. Controlled Release 5, 23–36.
Ritger, P.L., Peppas, N.A., 1987b. A simple equation for description of solute release II: Fickian and anomalous release from swellable devices. J. Controlled Release 5, 37–42.
Siepmann, J., Peppas, N.A., 2012. Modeling of drug release from delivery systems based on hydroxypropyl methylcellulose (HPMC). Adv. Drug Delivery Rev. 64, 163–174.
Song, L., Shen, Y., Hou, J., Lei, L., Guo, S., Qian, C., 2011a. Polymeric micelles for parenteral delivery of curcumin: preparation: characterization and in vitro evaluation. Colloids Surf. 390, 25–32.
Song, Z.M., Feng, R.L., Sun, M., Guo, C.Y., Gao, Y., Li, L.B., Zhai, G.X., 2011b. Curcumin-loaded PLGA-PEG-PLGA triblockcopolymeric micelles: preparation, pharmacokinetics and distribution in vivo. J. Colloid Interface Sci. 354, 116–123.
Tonnesen, H.H., 2002. Solubility, chemical and photochemical stability of curcumin in surfactant solutions – studies of curcumin and curcuminolds, XXVIII. Pharmazie 57, 820–824.
Torchilin, V.P., 2001. Structure and design of polymeric surfactant-based drug delivery systems. J. Controlled Release 73, 137–172.
Watanabe, M., Kawano, K., Yokoyama, M., Opanasopit, P., Okano, T., Maitani, Y., 2006. Preparation of camptothecin-loaded polymeric micelles and evaluation of their incorporation and circulation stability. Int. J. Pharm. 308, 183–189.
Wei, H., Cheng, S.X., Zhang, X.Z., Zhuo, R.X., 2009. Thermo-sensitive polymeric micelles based on poly(*N*-isopropylacrylamide) as drug carriers. Prog. Polym. Sci. 34, 893–910.
Xiao, K., Li, Y.P., Luo, J.T., Lee, J.S., Xiao, W.W., Gonik, A.M., Agarwal, R.G., Lam, K.S., 2011. The effect of surface charge on in vivo biodistribution of PEG-oligocholic acid based micellar nanoparticles. Biomaterials 32, 3435–3446.
Xu, F., Zheng, S.Z., Luo, Y.L., 2013. Thermosensitive *t*-PLA-*b*-PNIPAAm tri-armed star block copolymer nanoscale micelles for camptothecin drug release. J. Polym. Sci. Part A: Polym. Chem. 51, 4429–4439.
Yamamoto, Y., Nagasaki, Y., Kato, Y., Sugiyama, Y., Kataoka, K., 2001. Long-circulating poly(ethylene glycol)-poly(D,L-lactide) block copolymer micelles with modulated surface charge. J. Controlled Release 77, 27–38.
Yan, Y., Such, G.K., Johnston, A.P.R., Best, J.P., Caruso, F., 2012. Engineering particles for therapeutic delivery: prospects and challenges. ACS Nano 6, 3663–3669.
Yang, L., El Ghzaoui, A., Li, S.M., 2010a. In vitro degradation behavior of poly(lactide)-poly(ethylene glycol) block copolymer micelles in aqueous solution. Int. J. Pharm. 400, 96–103.
Yang, L., Qi, X., Liu, P., El Ghzaoui, A., Li, S.M., 2010b. Aggregation behavior of self-assembling polylactide/poly(ethylene glycol) micelles for sustained drug delivery. Int. J. Pharm. 394, 43–49.
Yang, R.L., Zhang, S.A., Kong, D.L., Gao, X.L., Zhao, Y.J., Wang, Z., 2012. Biodegradable polymer–curcumin conjugate micelles enhance the loading and delivery of low-potency curcumin. Pharm. Res. 29, 3512–3525.
Yokoyama, M., Okano, T., Sakurai, Y., Ekimoto, H., Shibazaki, C., Kataoka, K., 1991. Toxicity and antitumor activity against solid tumors of micelle-forming polymeric anticancer drug and its extremely long circulation in blood. Cancer Res. 51, 3229–3236.
Zhao, H.Z., Yung, L.Y.L., 2008. Selectivity of folate conjugated polymer micelles against different tumor cells. Int. J. Pharm. 349, 256–268.